Published in final edited form as:
Invest Radiol. 2001 March ; 36(3): 178.

Compartmental Modeling of Technetium-99m–Labeled Teboroxime with Dynamic Single-Photon Emission Computed Tomography:

Comparison with Static Thallium-201 in a Canine Model

Edward V. R. Di Bella, PhD, **Steven G. Ross, PhD**, **Dan J. Kadrmas, PhD**, **Harshali S. Khare, BS**, **Paul E. Christian, BS**, **Scott McJames, BS**, and **Grant T. Gullberg, PhD**
From the Medical Imaging Research Laboratory, Department of Radiology, University of Utah, Salt Lake City, Utah. Dr. Ross is now at GE Medical Systems, Waukesha, Wisconsin.

Abstract

RATIONALE AND OBJECTIVES—A compartmental modeling approach to deriving kinetic parameters from a time series of single-photon emission computed tomography (SPECT) images of technetium-99m–labeled (^{99m}Tc-) teboroxime may have value for semiquantitative assessment of myocardial perfusion. This study investigated the value of the kinetic parameters derived from a two-compartment model of ^{99m}Tc-teboroxime for measuring myocardial perfusion and compared it with static thallium-201 (^{201}Tl) uptake and microsphere-measured blood flow in dogs.

METHODS—Experiments were successfully conducted in 9 of 11 open-chest dogs. During adenosine stress, a single complete set of projections of ^{201}Tl uptake was acquired. ^{99m}Tc-teboroxime was then injected during adenosine stress, and a complete set of projections was acquired every 5.7 seconds for 17 minutes. Resting studies were performed on 4 of the animals. All of the projection sets were reconstructed with an iterative algorithm and incorporated corrections for attenuation and the geometric response of the collimators. Regional kinetic parameters (washin and washout) were determined semiautomatically from the time series of reconstructed ^{99m}Tc-teboroxime images and registered with microsphere data. Regional washin estimates were compared with ^{201}Tl intensities and myocardial blood flows determined from microspheres.

RESULTS—Optimally scaled ^{99m}Tc-teboroxime washin parameters and ^{201}Tl uptakes were correlated with microsphere-determined blood flows ($r = 0.91$, $y = 0.\ 99x + 1\ 0.01$, and $r = 0.92$, $y = 0.88x + 0.28$, respectively). In six of the studies, the left anterior descending coronary artery was occluded, and stress occluded-to-normal (O/N) ratios were calculated. The O/N ratios were 0.32 ± 0.17 as determined from microspheres injected with ^{201}Tl and 0.38 ± 0.29 from microspheres injected with ^{99m}Tc-teboroxime (P = NS). The O/N ratios were 0.48 ± 0.16 for static ^{201}Tl uptake and 0.27 ± 0.21 for ^{99m}Tc-teboroxime washin ($P < 0.05$).

CONCLUSIONS—Both ^{201}Tl uptake and ^{99m}Tc-teboroxime kinetic parameters were well correlated with flow. The ^{99m}Tc-teboroxime washin parameters offer semiquantitative flow values and provide greater defect contrast than can be obtained with ^{201}Tl uptake values.

Keywords

Dynamic SPECT; myocardium; nuclear medicine

Reprint requests: Edward Di Bella, PhD, Medical Imaging Research Laboratory, University of Utah, 729 Arapeen Dr., Salt Lake City, UT 84108-1218; ed@ucair.med.utah.edu.

Myocardial perfusion imaging with thallium-201 (^{201}Tl) is widely used for the diagnosis of coronary artery disease. However, the higher dose that can be used with technetium-99m–labeled (^{99m}Tc-) tracers and their better energy for single-photon emission computed tomography (SPECT) imaging can result in improved image statistics compared with those of ^{201}Tl. ^{99m}Tc-teboroxime is a neutral lipophilic tracer that has been shown to outperform ^{201}Tl in terms of initial extraction. However, ^{99m}Tc-teboroxime can be difficult to image owing to its rapid washout from myocardial tissue and its uptake by the liver. The rapid washout can, in some ways, be considered an advantage: a complete stress/rest study can be performed in much less time than with ^{201}Tl. If comparable or superior blood flow measurements can be obtained from imaging with ^{99m}Tc-teboroxime, then the brevity of the ^{99m}Tc-teboroxime protocol provides a significant clinical advantage. Another possible clinical advantage is that it may be possible to obtain quantitative measures of myocardial blood flow by using ^{99m}Tc-teboroxime and compartment modeling.

Several researchers have directly compared ^{99m}Tc-teboroxime with ^{201}Tl by using static planar imaging,[1–4] serial acquisition of planar images,[5] static SPECT imaging,[6,7] and serial acquisition of SPECT images.[8,9] To date, no comparisons of static ^{201}Tl imaging with dynamic ^{99m}Tc-teboroxime SPECT acquisitions in a physiologically realistic two-compartment model have been performed. By accurately approximating the dynamic processes of the tracer and incorporating measurements of the input function, kinetic parameter estimates may provide better measures of clinically relevant parameters than are possible with static imaging.[10] It is also possible that the compartment modeling approach will be superior to methods that acquire the data as a time sequence of images but that do not use compartmental models, as in previous studies.[5,8,9] In this article, myocardial perfusion measurements by dynamic SPECT imaging of ^{99m}Tc-teboroxime and compartmental modeling are compared with measurements from static SPECT imaging of ^{201}Tl in dogs.

Materials and Methods

Animal Preparation

Eleven mongrel dogs (mean ± SD weight, 30.4 ± 7.9 kg) were studied. Each dog was initially anesthetized with 8 mg/kg Telazol (MWI Veterinary Supplies, Nampa, ID). The dogs were then intubated and anesthetized with oxygen mixed with halothane (1%–10%). Small doses (3 mL) of a muscle relaxant (pancuronium) were administered as needed. Heparin was administered at regular intervals. The chest was opened at the fifth left intercostal space and the heart suspended in a pericardial cradle. A catheter for microsphere delivery was placed in the left atrial appendage and secured with a purse-string suture. An ultrasonic flow probe was placed around the left anterior descending coronary artery (LAD) between the first and second diagonal branches. In 8 of the animals, the LAD was occluded before imaging. For these studies, either a snare ($n = 6$) or a hydraulic occluder ($n = 2$) was placed on the LAD just distal to the flow probe. The animal procedures were approved by the University of Utah's Institutional Animal Care and Use Committee.

Because scatter into the inferior wall from a "hot" liver can be problematic with ^{99m}Tc-teboroxime, gauze was placed above the liver to hold it away from the heart. This was done through an incision made in the abdomen. For clinical applications, it may be necessary to compensate for scatter with a sophisticated scatter-modeling technique[11] or to exclude liver effects with postreconstruction processing.[12]

Data Acquisition

A three-detector SPECT system (Marconi Medical Systems, Cleveland, OH) was used for all imaging. The experimental protocol is presented in timeline form in Figure 1; the order of the

protocol was changed in two of the animals (see Table 1). In the basic protocol, the animal was first secured in a right lateral decubitus position on the scanner, and a transmission scan was performed. Then vasodilation stress was induced with adenosine. Thallium-201 (1–4 mCi, or 37–148 MBq) was injected after blood flow (as measured by the LAD flow probe) had stabilized; adenosine infusion was continued. Imaging commenced 10 to 20 minutes after injection of ^{201}Tl. Projections of 30 seconds each were collected over 20 minutes.

The ^{99m}Tc-teboroxime scans followed the ^{201}Tl studies in all cases, so that downscatter from ^{99m}Tc-teboroxime into the ^{201}Tl energy window would not be an issue. Between 14 and 30 mCi (518–1100 MBq) of ^{99m}Tc-teboroxime was injected during adenosine stress, along with ruthenium-103 microspheres. The ^{99m}Tc-teboroxime acquisitions resulted in 179 sequential sets of projection data. Each set was acquired in 5.7 seconds by continuous rotation of the camera gantry. Adenosine infusion was continued until imaging of ^{99m}Tc-teboroxime was complete in all but two animals. In those two cases, adenosine was infused as it would be in human protocols: a 0.14 mg $\cdot$ kg^{-1} $\cdot$ min^{-1} infusion for 6 minutes, with injection at 3 minutes.

In four animals, resting ^{201}Tl and ^{99m}Tc-teboroxime scans were performed in addition to the stress scans (Table 1). The same imaging protocols were used as in the stress acquisitions.

Simultaneously with each of the radionuclide injections, approximately 1.3×10^6 radiolabeled microspheres (tin-113, ruthenium-103, cobalt-57, or scandium-46), 15 μm in diameter, were injected into the left atrium. An arterial reference sample was withdrawn at a rate of 7 mL/min during the microsphere injection. The withdrawal began before injection of the microspheres and continued for at least 90 seconds.

Of the 11 dogs, 1 went into fibrillation (probably due to an unusually large LAD occlusion) and died during the ^{201}Tl scan. In another animal, the occlusion became detached and the animal was hypotensive (mean arterial pressure = 50 mm Hg) during part of the study; data from this animal were excluded from analysis. In addition, 2 of the microsphere injections resulted in microsphere data that were incorrectly scaled—the microsphere reference withdrawal failed to acquire any microspheres, making the flow values an order of magnitude higher than physiologically possible. Although withdrawal was always started before microsphere injection, it is possible that blood was still present in the tubing at some point but was not noticeable. Thus, the appropriate scaling of the microsphere flow data were not known, so these 2 studies were used for occluded-to-normal (O/N) ratio results only. Thus, from the 26 studies listed in Table 1, 22 studies from 9 dogs were used when comparing microsphere-determined flows and ^{201}Tl uptake and ^{99m}Tc-teboroxime kinetic parameters.

At the conclusion of each study, the dog was sacrificed and the heart excised. When an occlusion had been in place, blue dye was injected into the LAD just below the occlusion to define the risk area. The heart tissue was then sectioned into approximately six 7-mm to 1-cm-thick slices. Each slice was photographed and cut into quadrants or eighths. The sections were weighed and well counted.

Data Processing and Analysis

The transmission maps were reconstructed with six iterations of ordered subsets–expectation maximization (OS-EM), postprocessed with a median filter, and scaled for the appropriate energies. A manually chosen subset of slices of the emission data encompassing the heart was chosen to be reconstructed because the computational demands were intensive. Both the ^{99m}Tc-teboroxime and the ^{201}Tl data were reconstructed with six iterations of the OS-EM algorithm, with attenuation correction and an accurate model of the depth-dependent point response arising from the geometry of the collimator. The short-axis slices were passed to a program that generated septal, anterior, lateral, and inferior regions of interest (ROIs) in each

slice, given the center point of each short-axis slice.[12] The resulting ROIs were visually aligned with photographs of the ex vivo short-axis slices. Manual adjustment of some of the ROIs was performed to better match the microsphere-containing regions. The average size of the ROIs was approximately 2.2 cm^3.

The ^{99m}Tc-teboroxime data were further processed to determine kinetic parameters by compartmental modeling. Compartmental modeling is based on the dynamics of the physiological process undergone by the tracer. Dynamic positron emission tomography and SPECT imaging aim to provide a quantitative measure of the parameters that describe the dynamics of a physiological process. The equation for the two-compartment model used is

$$A(t)=(1-f_v)k_{21}\int_t^{t+\Delta t} e^{-k_{12}t'} \times B(t')dt' + f_v\int_t^{t+\Delta t} B(t')dt'$$

where *A(t)* is the activity measured in an ROI, k_{21} is the washin parameter, k_{12} is the washout parameter, and the activity is integrated over the time required to collect a set of projections, Δt. *B(t)* is the time-activity curve of the blood input function. For the studies reported in this article, *B(t)* was estimated from an ROI placed on the left ventricular blood pool in the images. The parameter f_v is a free variable that allows modeling of the fraction of the blood in tissue (blood in capillaries as well as spillover from resolution and pixelization effects).

A blood ROI was chosen manually in a few slices between the midventricular slice and the most basal slice. The size of the blood ROI was approximately 4 cm^3. The blood and each regional tissue time-activity curve were fit to the two-compartment model given in Equation 1 by using RFIT (Center for Functional Imaging, E.O. Lawrence Berkeley National Laboratory, University of California, Berkeley, CA).[13] Parameters for washin (k_{21}), washout (k_{12}), and the fraction of blood in the tissue (f_v) were found for each region.

Microsphere data were used to determine regional myocardial blood flow according to the procedure of Heymann et al.[14] This method includes correction for cross-contamination of the different energy windows. Technetium-99m–teboroxime washin parameters and ^{201}Tl uptakes were then scaled, so that the average of the washins or uptakes in the regions corresponding to those that were well counted was equal to the average of that study's microsphere-determined blood flow. Correlations with microsphere blood flow data were then computed. Because this interstudy scaling can create artificially high correlations, regressions were also computed for unscaled washin parameters and for ^{201}Tl scaled by dose (mCi/kg).

O/N Ratios

Six studies with the LAD occluded were performed under adenosine stress. For these studies, ROIs of the occluded region were chosen manually in the anteroseptal region. ROIs distant from the occluded region were chosen to define the normal region. Washin (k_{21}) and washout (k_{12}) values were determined for the occluded region and the normal region, and O/N ratios were calculated. Average ^{201}Tl uptake values in the occluded and normal regions were used to determine the O/N ratios for ^{201}Tl.

A similar procedure was followed to determine O/N ratios from microsphere-based flow measurements. In this case, the occluded region was chosen from the blue-stained areas of the photographs and microsphere-determined flows.

Statistical Tests

Correlation coefficients of the washin of ^{99m}Tc-teboroxime to microsphere flow and uptake of ^{201}Tl to microsphere flow were calculated. Significance of the correlations was tested by

the null hypothesis that there was no linear relationship between the different methods of measuring flow ($r = 0$); if $P < 0.05$, the conclusion that there was a significant correlation was made. Differences between O/N ratios were calculated by using a two-tailed, paired *t* test.

Results

Correlations and Regressions

The relationships between the microsphere flow measurements and SPECT imaging results, when 20 quarter-of-a-slice regions were used as the ROIs in 11 studies for each radionuclide (220 data points), are plotted in Figure 2, and these results are summarized in Table 2.

Correlations within studies were also examined to avoid scaling issues. These intrastudy correlations are reported in Table 3. The studies reported in Table 3 are all from different animals except for studies 4 and 6, which were performed on the same animal. Although the correlation coefficients are not high, most of the studies achieve a significant ($P < 0.05$) relationship between microsphere-measured blood flow and ^{201}Tl and ^{99m}Tc-teboroxime. Note that studies of unoccluded myocardium (rows 1 and 2 in Table 3) are not expected to have high correlations.

O/N Ratios

The O/N ratios for the six stress studies are reported in Table 4. The O/N ratios from microsphere-determined flows were 0.32 ± 0.17 from microspheres injected with ^{201}Tl and 0.38 ± 0.29 from microspheres injected with ^{99m}Tc-teboroxime (P = NS). The contrast between the ischemic and normal zones was significantly greater with the ^{99m}Tc-teboroxime washin parameters than with ^{201}Tl, but contrast from washout parameters was not significantly different from that with ^{201}Tl.

Discussion

Radionuclide Imaging

Although previously published comparisons between ^{201}Tl and ^{99m}Tc-teboroxime did not use compartmental modeling methods, imaging with ^{99m}Tc-teboroxime has been reported to have clinical utility comparable to ^{201}Tl in many cases. Bontemps et al[2] found that using ^{99m}Tc-teboroxime with a static planar imaging protocol gave a sensitivity comparable to that obtained with ^{201}Tl for detecting coronary artery disease. The specificity of ^{99m}Tc-teboroxime was reported by Bontemps et al[2] to be improved over that of ^{201}Tl (77% vs. 60%). Similar results in 30 patients have been reported as well.[1] Serially acquired planar studies comparing ^{99m}Tc-teboroxime and ^{201}Tl in swine[5] have also shown the potential utility of ^{99m}Tc-teboroxime. Single-photon emission computed tomography imaging with ^{99m}Tc-teboroxime has been reported to be very promising in comparison to ^{201}Tl SPECT.[6] Weinstein et al[15] reported that in rabbits, ^{99m}Tc-teboroxime may be better than ^{99m}Tc-sestamibi and ^{201}Tl in terms of contrast and sizing of hypoperfused myocardium. Di Rocco et al[16] compared ^{99m}Tc-teboroxime, ^{201}Tl, and ^{96}Tc-sestamibi in rats and dogs by well counting. A “snapshot” of ^{99m}Tc-teboroxime distribution at 70 seconds postinjection was shown to reflect flow more accurately than did ^{201}Tl in rats and was comparable to ^{201}Tl flows in dogs.

Many studies have focused on the washout phase of the ^{99m}Tc-teboroxime tracer,[4,17] as the washin is extremely rapid. Ex vivo planar imaging comparisons have been done between ^{99m}Tc-teboroxime and ^{201}Tl uptake at 2 minutes postinjection in dogs.[18] In that study, ^{99m}Tc-teboroxime did not reflect microsphere-measured myocardial blood flow as well as did ^{201}Tl. That is, the O/N ratios from ^{99m}Tc-teboroxime showed less contrast than did either ^{201}Tl or microsphere-determined flow. Sufficiently rapid acquisitions, however, have

shown that the washin of ^{99m}Tc-teboroxime is correlated with microsphere-measured blood flow. Stewart et al[19] investigated the washout rates of ^{99m}Tc-teboroxime in open-chest dogs by using a sodium iodide probe and a ring SPECT system. They found the washout measured with the sodium iodide probe to be correlated with microsphere-measured flows. Chiao et al[20] and Smith et al[10] improved the methods of Stewart et al by using tracer kinetic compartmental models in humans and dogs, respectively. Chiao et al[20] found in normal volunteers that k_{21} and washout (not compartmental modeling washout) values were correlated but that k_{21} stress/rest ratios and non-compartmental model washout stress/rest ratios were not correlated significantly. Of note is that attenuation correction was not performed in the study by Chiao et al. Smith et al[10] found significant correlations between ^{99m}Tc-teboroxime compartmental model washin values from large regions of the left ventricle and microsphere-determined blood flows in dogs. The work in the current study used reconstruction methods different from those of Smith et al and region sizes that could be clinically useful—a quarter of a short-axis slice, rather than a quarter of the left ventricle—as used by Smith et al.[10]

Static ^{99m}Tc-teboroxime (acquired in a dynamic manner to minimize inconsistencies in the projection data) has been found to not be correlated with blood flow as well as are the washin estimates.[21] Given the results from well-counting experiments in Glover et al18 and Beanlands et al,22 static ^{99m}Tc-teboroxime will also not likely provide as great an O/N contrast as does dynamic imaging with compartmental modeling.

Correlation and Regression Analysis

Data from regions of the left ventricle of a clinically useful size revealed that both ^{201}Tl uptake and ^{99m}Tc-teboroxime washin parameters were correlated highly with microsphere-measured blood flow and with each other ($y = 1.4x - 0.38$; $r = 0.79$). Note that the data were “optimally” scaled to microsphere-measured flows. The scaling method chosen has the effect of creating an artificial correlation such that the sum of each study is correlated perfectly with microsphere measurements. Correlations using smaller regions are less affected. Some sort of scaling is essential for ^{201}Tl; otherwise, uptake differences between studies result in ^{201}Tl uptakes that are not correlated with flow. Other methods (eg, dividing by mCi/kg or normalizing both ^{201}Tl and microsphere values to their means or maxima23) for normalizing the ^{201}Tl data were explored but resulted in much less agreement with microsphere data (Table 2). In contrast, ^{99m}Tc-teboroxime washin and washout parameters were correlated with microsphere-determined flows when no scaling was used. This semiquantitative nature of the kinetic parameters is potentially of value in numerous applications.

The regression plot for ^{99m}Tc-teboroxime washin and washout parameters in Figure 3 displays more scatter of the data about the line of regression at high flows than does the corresponding regression plot of ^{201}Tl uptake. The implication for clinical imaging is that the large standard deviation of the measurements may cause difficulty in distinguishing abnormal from normal flow regions. However, this scatter at high flow was largely due to a single study; Figure 4 shows the washin regression plot with this study excluded ($y = 0.89x + 0.28$; $r = 0.89$).

Previously published results have shown ^{201}Tl and ^{99m}Tc-teboroxime to have similar relationships to microsphere flows at 70 seconds postinjection.[16] The study by Di Rocco et al[16] used well counting rather than imaging for both ^{99m}Tc-teboroxime and ^{201}Tl; it is unwise to extrapolate this relationship to SPECT imaging results. Comparison of O/N ratios (below) provides a means of normalization, so results can be compared more rigorously.

O/N Ratios

The O/N ratios (Table 4) show that the ^{99m}Tc-teboroxime washin parameters tended to provide greater contrast between the occluded and normal zones than did the ^{201}Tl uptake values. This

finding is consistent with reports in the literature that autoradiographic images of ^{99m}Tc-teboroxime provide more contrast and reflect larger hypoperfused areas than does ^{201}Tl or ^{99m}Tc-sestamibi.[15] Because gauze was placed superior to the liver to hold it away from the heart, scatter due to liver activity should not have played a significant role in the O/N ratios calculated. However, scatter from other sources affected both radionuclides and likely contributed to the decreased contrast found in the O/N ratios for ^{201}Tl in particular. Washout O/N ratios give much less contrast than do washin parameters.

In Table 4, study 4, the ^{99m}Tc-teboroxime data have a lower O/N ratio than do the microsphere data (0.05 vs. 0.16), implying that the washin parameters show greater contrast. However, similar contrast is seen in the images (not shown). This is because small changes (noise) of the values in the occluded region can be misleading when values in the occlusion region approach zero. The actual range (maximum-minimum) of flow values from the ^{99m}Tc-teboroxime and microsphere studies, when both are scaled to a common maximum, are similar (2.9 and 2.6, respectively).

Limitations

The blood input function must be accurately estimated because the use of a compartmental model assumes that the time-varying activity concentration in the tissue compartment is the convolution of the activity in the blood compartment with some function of the kinetic parameters. Extravascular contamination of the blood input function has been shown to be on the order of 45% in dogs when the blood pool is chosen manually.[10] This level of contamination can potentially bias washin estimates by 75%.[24] This implies that the correlations reported here between ^{99m}Tc-teboroxime and microsphere flow can be improved if more accurate blood input functions can be obtained.

One assumption of the two-compartment model is that the extraction fraction of ^{99m}Tc-teboroxime in the myocardium is constant during the time of measurement. This assumption is not valid,[25] since teboroxime binds to blood and has an extraction fraction that decreases rapidly after the first pass. Binding to blood components was addressed briefly by Chiao et al[20] but was reported not to be a major concern, since the data fit two compartments well. It is possible that binding, being the same for all regions, only scales k_{21} globally; relative k_{21} values may still be useful. Stewart et al[19] also reported that blood activity decreased quickly after intravenous injection. At 2 minutes postinjection, activity was 8% of peak, implying that binding would need to be very rapid to significantly affect ^{99m}Tc-teboroxime uptake.[22]

Clinical studies are underway at our institution to determine whether dynamic SPECT imaging of teboroxime is useful in humans. The clinical protocol differs little from standard myocardial perfusion imaging, except that timing is more critical and a series of projection sets are acquired. We note that immediately sequential rapid tomographic acquisitions are not feasible for all scanners; this may not be an issue with further development of methods for estimation of kinetic parameters from projection data.[26]

Conclusions

Regional kinetic parameters derived from dynamic SPECT ^{99m}Tc-teboroxime images are correlated with microsphere-determined blood flow but have characteristics different from those of ^{201}Tl. Dynamic SPECT imaging of ^{99m}Tc-teboroxime with a two-compartment model tends to provide greater contrast between occluded and normal myocardium than do ^{201}Tl intensities and more closely matches microsphere-derived flow ratios. Without scaling, ^{99m}Tc-teboroxime kinetic parameters still provided reasonable correlations to microsphere flow data. This semiquantitative property may enable follow-up studies to be compared to determine the effects of therapy. Furthermore, with incorporation of practical

compensations for scatter and partial-volume effects and development of methods for more accurate noninvasive estimation of the blood input function, quantitative blood flow measurements in clinically useful region sizes may be possible.

Acknowledgments

The authors thank Albert J. Sinusas, MD (Yale University) for his help with animal study methodology, and Eric C. Frey, PHD (University of North Carolina, Chapel Hill) for his help with reconstruction software.

This work has been supported by National Institutes of Health grant R01 HL50663.

References

1. Seldin DW, Johnson LL, Blood DK, et al. Myocardial perfusion imaging with technetium-99m SQ30217: Comparison with thallium-201 and coronary anatomy. J Nucl Med 1989;30:312–319. [PubMed: 2738660]
2. Bontemps L, Geronicola-Trapali X, Sayegh Y, et al. Technetium-99m teboroxime scintigraphy. Eur J Nucl Med 1991;18:732–739. [PubMed: 1936049]
3. Taillefer R, Lambert R, Esseiambre R, et al. Comparison between thallium-201, technetium-99m-sestamibi and technetium-99m-teboroxime planar myocardial perfusion imaging in detection of coronary artery disease. J Nucl Med 1992;33:1091–1098. [PubMed: 1534575]
4. Hendel RC, Dahlberg ST, Weinstein H, et al. Comparison of teboroxime and thallium for the reversibility of exercise-induced myocardial perfusion defects. Am Heart J 1993;126:856–862. [PubMed: 8213442]
5. Gray WA, Gewirtz H. Comparison of 99m-Tc-teboroxime with thallium for myocardial imaging in the presence of a coronary artery stenosis. Circulation 1991;84:1796–1807. [PubMed: 1914115]
6. Drane WE, Keim S, Strickland P, et al. Preliminary report of SPECT imaging with Tc-99m teboroxime in ischemic heart disease. Clin Nucl Med 1992;17:215–225. [PubMed: 1611794]
7. Serafini AN, Topchik S, Jimenez H, et al. Clinical comparison of technetium-99m-teboroxime and thallium-201 utilizing a continuous SPECT imaging protocol. J Nucl Med 1992;33:1304–1311. [PubMed: 1613570]
8. Chua T, Kiat H, Germano G, et al. Rapid back to back adenosine stress/rest technetium-99m teboroxime myocardial perfusion SPECT using a triple-detector camera. J Nucl Med 1993;34:1485–1493. [PubMed: 8355068]
9. Chua T, Kiat H, Germano G, et al. Technetium-99m teboroxime regional myocardial washout in subjects with and without coronary artery disease. Am J Cardiol 1993;72:728–734. [PubMed: 8249853]
10. Smith AM, Gullberg GT, Christian PE. Experimental verification of technetium-99m-labeled teboroxime kinetic parameters in the myocardium with dynamic single-photon emission computed tomography: Reproducibility, correlation to flow, and susceptibility to extravascular contamination. J Nucl Cardiol 1996;3:130–142. [PubMed: 8799238]
11. Frey, EC.; Tsui, BMW. A new method for modeling the scatter response function in SPECT. IEEE Med Imaging Conf; 1996. p. 1082-1086.
12. Di Bella EVR, Gullberg GT, Barclay AB, et al. Automated region selection for analysis of dynamic cardiac SPECT data. IEEE Trans Nucl Sci 1997;44:1355–1361.
13. Huesman, RH.; Knittel, BL.; Mazoyer, BM., et al. Notes on RFIT: A program for fitting compartment models to region-of-interest dynamic emission tomography data. version 4.4 edition. Berkeley, CA: Lawrence Berkeley Laboratory; 1995. publication No. LBL-37621
14. Heymann MA, Payne BD, Hoffman JIE, et al. Blood flow measurements with radionuclide-labeled particles. Prog Cardiovasc Dis 1977;20:55–79. [PubMed: 877305]
15. Weinstein H, Reinhardt CP, Leppo JA. Teboroxime, sestamibi, and thallium-201 as markers of myocardial hypoperfusion: Comparison by quantitative dual-isotope autoradiography in rabbits. J Nucl Med 1993;34:1510–1517. [PubMed: 8355072]

16. DiRocco RJ, Rumsey WL, Kuczynski BL, et al. Measurement of myocardial blood flow using a co-injection technique for technetium-99m-teboroxime, technetium-96-sestamibi and thallium-201. J Nucl Med 1992;33:1152–1159. [PubMed: 1534576]

17. Stewart RE, Heyl B, O'Rourke RA, et al. Demonstration of differential post-stenotic myocardial technetium-99m-teboroxime clearance kinetics after experimental ischemia and hyperemic stress. J Nucl Med 1991;32:2000–2008. [PubMed: 1919745]

18. Glover DK, Ruiz M, Bergmann EE, et al. Myocardial technetium-99m-teboroxime uptake during adenosine-induced hyperemia in dogs with either a critical or mild coronary stenosis: Comparison to thallium-201 and regional blood flow. J Nucl Med 1995;36:476–483. [PubMed: 7884514]

19. Stewart RE, Schwaiger M, Hutchins GD, et al. Myocardial clearance kinetics of technetium-99m-SQ30217: A marker of regional myocardial blood flow. J Nucl Med 1990;31:1183–1190. [PubMed: 2362197]

20. Chiao P-C, Ficaro EP, Dayanikli F, et al. Compartmental analysis of technetium-99m-teboroxime kinetics employing fast dynamic SPECT at rest and stress. J Nucl Med 1994;35:1265–1273. [PubMed: 8046477]

21. Kadrmas DJ, Di Bella EVR, Khare HS, et al. Static versus dynamic teboroxime myocardial perfusion SPECT in canines. IEEE Trans Nucl Sci 2000;47:1112–1117. [PubMed: 20090867]

22. Beanlands R, Muzik O, Nguyen N, et al. The relationship between myocardial retention of technetium-99m teboroxime and myocardial blood flow. J Am Coll Cardiol 1992;20:712–719. [PubMed: 1512353]

23. Meleca MJ, McGoron AJ, Gerson MC, et al. Flow versus uptake comparisons of thallium-201 with technetium-99m perfusion tracers in a canine model of myocardial ischemia. J Nucl Med 1997;38:1847–1856. [PubMed: 9430457]

24. Smith AM, Gullberg GT. Dynamic cardiac SPECT computer simulations for teboroxime kinetics. IEEE Trans Nucl Sci 1994;41:1626–1633.

25. Rumsey WL, Rosenspire KC, Nunn AD. Myocardial extraction of teboroxime: Effects of teboroxime interaction with blood. J Nucl Med 1992;33:94–101. [PubMed: 1530970]

26. Reutter BW, Gullberg GT, Huesman RH. Direct least squares estimation of spatiotemporal distributions from dynamic SPECT projections using a spatial segmentation and temporal B-splines. IEEE Trans Med Imaging 2000;19:434–450. [PubMed: 11021687]

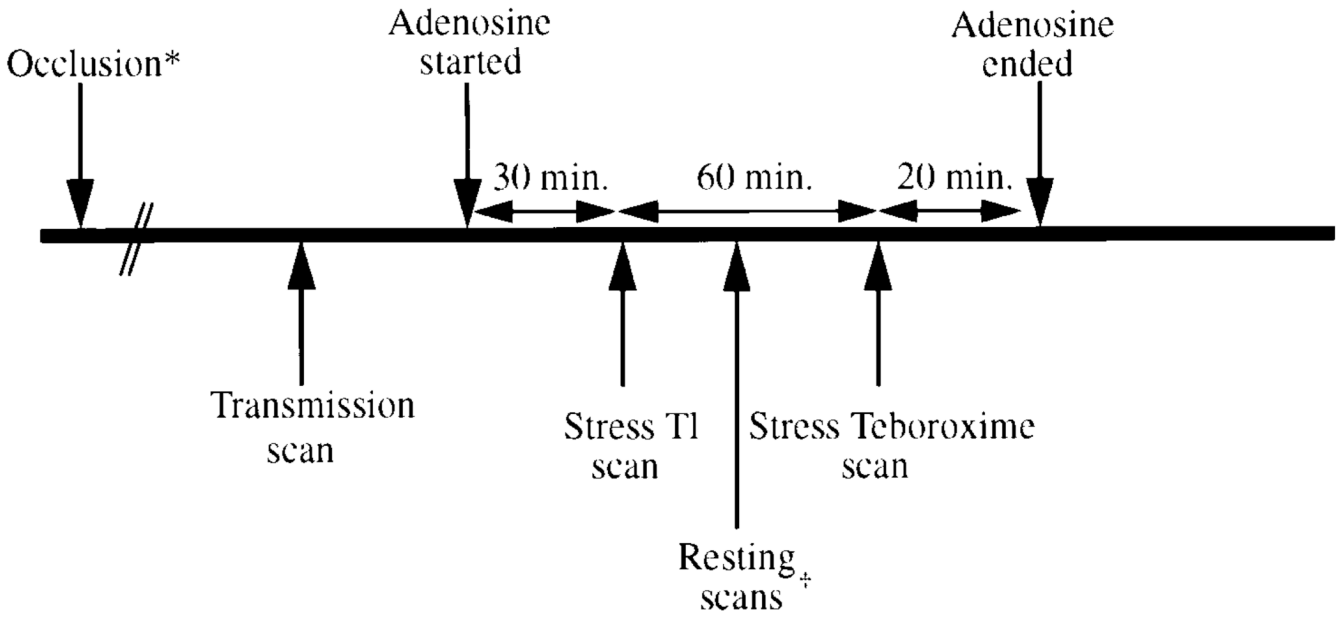

Figure 1.
Experimental protocol. The *asterisk* (*) denotes that occlusion was performed in six of the nine studies, and the *dagger* (†) denotes that resting ^{201}Tl was performed in four studies. See also Table 1.

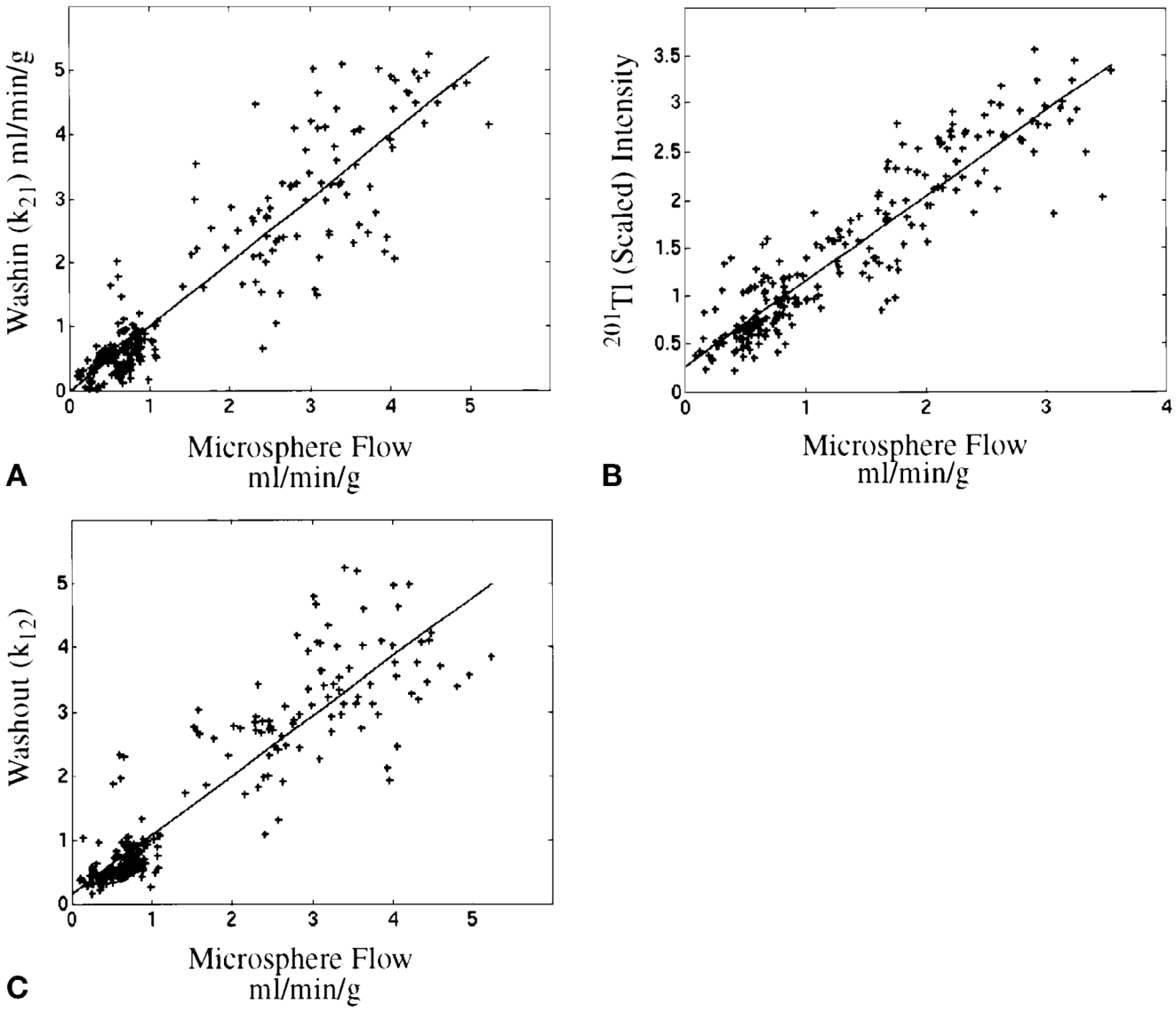

Figure 2.

Regression lines for data from 220 regions from 11 studies in nine dogs. (A) Microsphere flows vs. washin: $r = 0.91$ ($y = 0.99x + 0.01$). (B) Microsphere flows vs. ^{201}Tl: $r = 0.92$ ($y = 0.88x + 0.28$). (C) Microsphere flows vs. washout: $r = 0.91$ ($y = 0.89x + 0.26$). In all cases shown here, the kinetic parameters and ^{201}Tl uptakes were each scaled to match the average of microsphere-derived flows in each study.

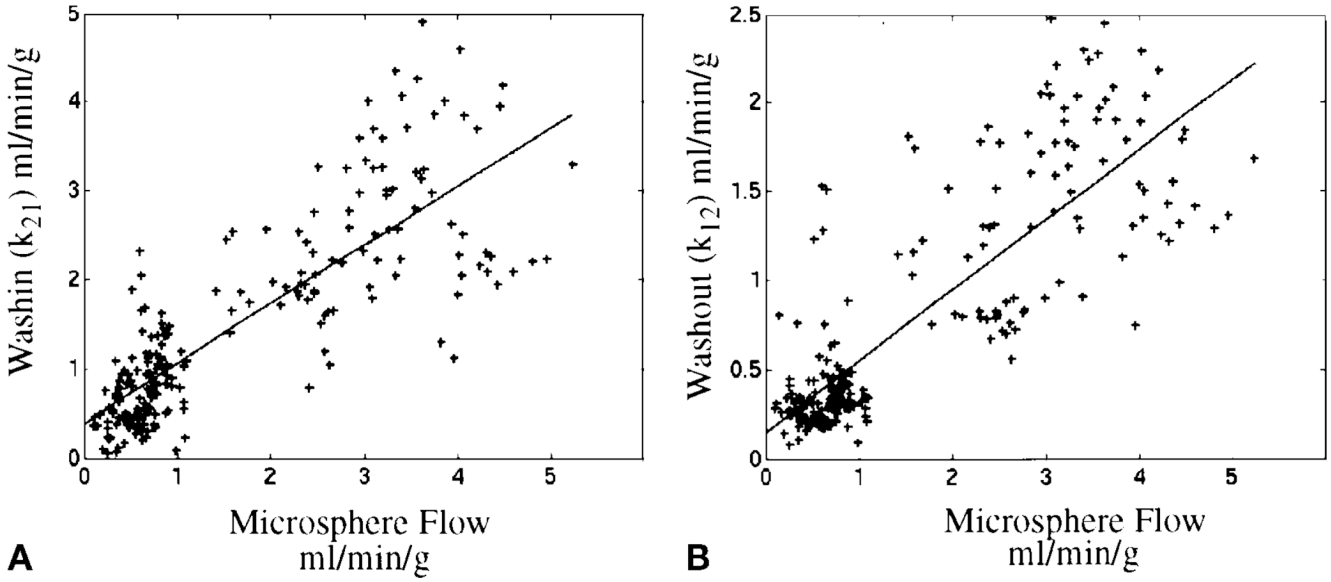

Figure 3.
Plots in (A) and (B) are the same as those in Figures 2A and 2C, respectively, except here the kinetic parameters were not scaled before comparison with microsphere-derived flow values.

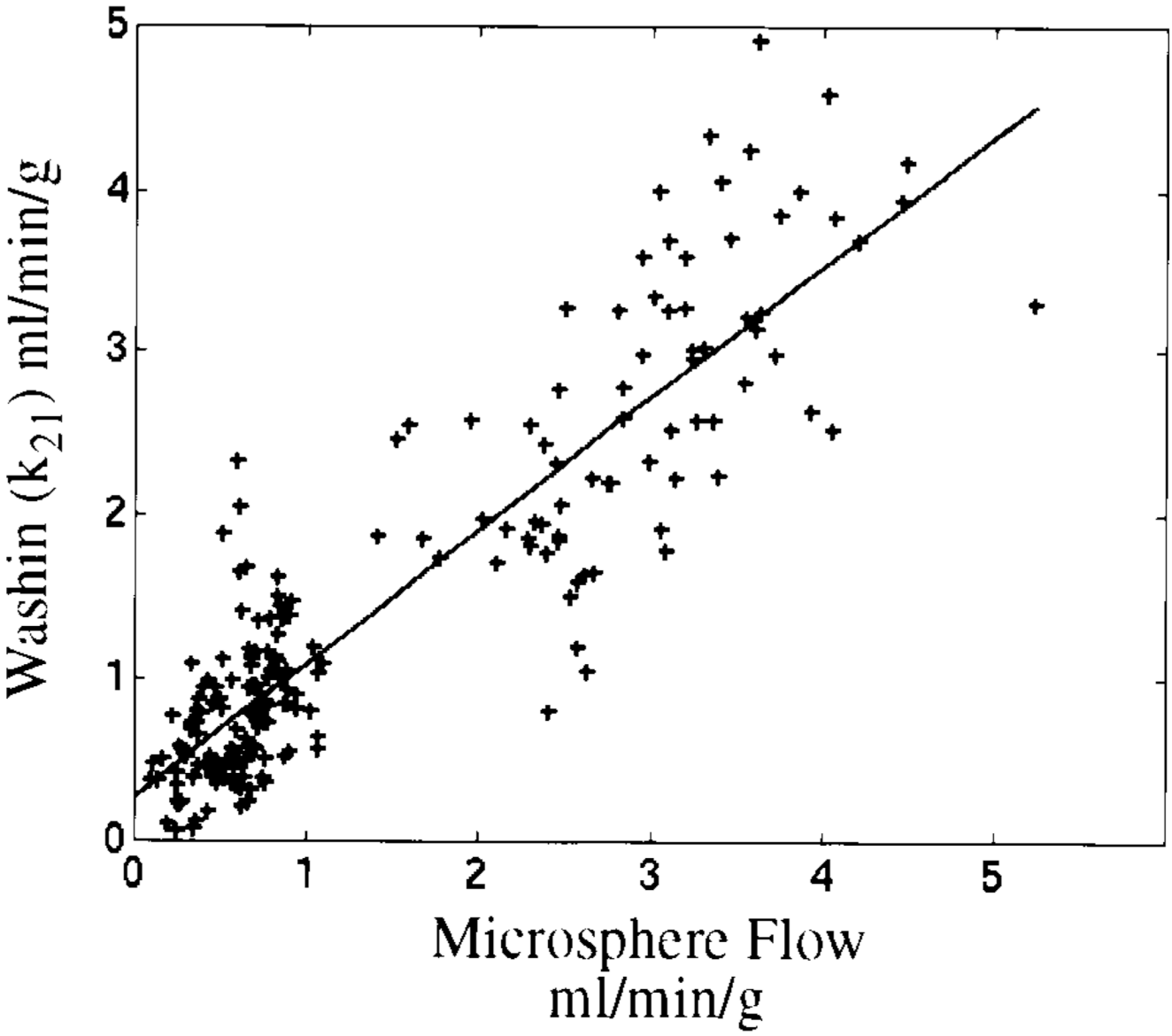

Figure 4.
The study shown is the same as in Figure 3A but without the outlying study. The correlation coefficient for unscaled washin improved to $r = 0.89$. See text in the Discussion section for details.

TABLE 1

Summary of Canine Experiments

Animal no.	Imaging protocol	Occlusion
1	1: Tl stress; 2: Teb. stress	None
2	1: Tl stress; 2: Teb. stress	None
3	1: Tl stress; 2: Teb. stress	Hydraulic
4	1: Tl stress; 2: Teb. stress	Snare
5	1: Tl stress; 2: Tl rest; 3: Teb. rest; 4: Teb. stress	Snare
6	1: Tl stress; 2: Teb. stress	Hydraulic
7	1: Tl stress; 2: Tl rest; 3: Teb. rest; 4: Teb. stress	None
8	1: Tl rest; 2: Tl stress; 3: Teb. rest; 4: Teb. stress	Snare
9	1: Tl rest; 2: Tl stress; 3: Teb. rest; 4: Teb. stress	Snare

Teb. indicates ^{99m}Tc-teboroxime; Tl: thallium-201.

TABLE 2

Interstudy Correlations and Fits (see Fig. 2)

Study	*r*	Fit equation
Tl vs. flow	0.92	$y = 0.88x + 0.28$
Teb. washin vs. flow	0.91	$y = 0.99x + 0.01$
Teb. washout vs. flow	0.91	$y = 0.89x + 0.26$
Tl (scaled by mCi/kg) vs. flow	0.14	…
Teb. washin (unscaled) vs. flow	0.82	$y = 0.66x + 0.41$
Teb. washout (unscaled) vs. flow	0.83	$y = 0.40x + 0.15$
Teb. washin (unscaled) vs. Tl	0.81	$y = 1.1x - 0.03$
Teb. washout (unscaled) vs. Tl	0.69	$y = 0.54x + 0.02$

Teb. indicates ^{99m}Tc-teboroxime; Tl: thallium-201.

TABLE 3

Intrastudy Correlations for 20 Regions

Study	Tl vs. spheres	Teb. vs. spheres	Teb. vs. Tl
1 (stress)	0.54	0.71	0.42*
2 (stress)	0.45	0.62	0.88
4 (stress)	0.76	0.80	0.89
5 (rest)	0.46	0.26*	0.92
6 (stress)	0.25*	0.44	0.36*
7 (rest)	0.56	0.30*	0.94
7 (stress)	0.56	0.43*	0.66
8 (rest)	0.79	0.75	0.81
8 (stress)	0.79	0.56	0.76
9 (rest)	0.72	0.79	0.92
9 (stress)	0.77	0.75	0.95
Mean ± SD	0.61 ± 0.18	0.58 ± 0.20	0.77 ± 0.21

Tl indicates thallium-201; Teb.: ^{99m}Tc-teboroxime.

Cutoff for significance ($P < 0.05$) is $r = 0.44$

*(indicates not significant).

TABLE 4

O/N Ratios at Stress

Study No. (from Table 1)	O/N Tl spheres	O/N Tl	O/N teboroxime spheres	O/N teboroxime washin	O/N teboroxime washout
3	0.42	0.63	0.85	0.55	0.81
4	0.24	0.46	0.20	0.08	0.14
5	0.04	0.26	0.02	0.06	0.53
6	0.49	0.58	0.44	0.45	0.51
8	0.44	0.63	0.30	0.36	0.94
9	0.27	0.32	0.50	0.14	0.51
Mean ± SD	0.32 ± 0.17	0.48 ± 0.16	0.38 ± 0.29	0.27 ± 0.21	0.57 ± 0.28

O/N indicates occluded to normal; Tl: thallium-201.